Spontaneous Orbital-Selective Mott Transitions and the Jahn-Teller Metal of A_3C_{60}

Shintaro Hoshino[1] and Philipp Werner[2]
[1]RIKEN Center for Emergent Matter Science (CEMS), Wako, 351-0198 Saitama, Japan
[2]Department of Physics, University of Fribourg, 1700 Fribourg, Switzerland
(Received 11 September 2016; published 28 April 2017)

The alkali-doped fullerides A_3C_{60} are half-filled three-orbital Hubbard systems which exhibit an unconventional superconducting phase next to a Mott insulator. While the pairing is understood to arise from an effectively negative Hund coupling, the highly unusual Jahn-Teller metal near the Mott transition, featuring both localized and itinerant electrons, has not been understood. This property is consistently explained by a previously unrecognized phenomenon: the spontaneous transition of multiorbital systems with negative Hund coupling into an orbital-selective Mott state. This symmetry-broken state, which has no ordinary orbital moment, is characterized by an orbital-dependent two-body operator (the double occupancy) or an orbital-dependent kinetic energy and may be regarded as a diagonal-order version of odd-frequency superconductivity. We propose that the recently discovered Jahn-Teller metal phase of $Rb_xCs_{3-x}C_{60}$ is an experimental realization of this novel state of matter.

DOI: 10.1103/PhysRevLett.118.177002

The appearance of long-range order by spontaneous symmetry breaking (SSB) is a fundamental and widely studied concept in physics. In condensed matter systems, the ordered state is typically characterized by an order parameter measuring the charge, magnetic moment, orbital angular momentum, or the pair amplitude in a superconductor. There may, however, exist more complex types of ordering phenomena. Here we demonstrate that in a certain class of multiorbital systems one observes an orbital symmetry breaking into a state without a conventional order parameter but with an orbital-dependent double occupancy (a composite order parameter) and an orbital-dependent kinetic energy. The resulting ordered phase is a spontaneous orbital-selective Mott (SOSM) state, in which itinerant and localized electrons coexist. As this state combines properties of the metal (connected to the weak-interaction limit) and Mott insulator (connected to the strong-interaction limit), it cannot be detected by perturbative methods from either limit, and its study requires the use of sophisticated techniques. The ordering phenomenon can be discussed in terms of a symmetry-breaking field or order parameter with odd time (frequency) dependence and is hence related to the concept of odd-frequency superconductivity [1–4].

We will argue that this unconventional SOSM state is realized in alkali-doped fullerides [5–13], which are promising candidates for diagonal odd-frequency orders. Several compounds in this class of materials can be regarded as strongly correlated systems, since a Mott transition occurs as a function of pressure. In the case of an fcc lattice [12], the Mott insulator stays paramagnetic in a wide range of temperatures due to geometrical frustration, while it is antiferromagnetically ordered in the case of a bcc lattice, which is bipartite [11]. With increasing pressure, the system turns into a paramagnetic metal and is unstable to superconductivity below a maximum $T_c \simeq 38$ K [11]. Recently, a so-called Jahn-Teller metal (JTM) state has been experimentally identified in fcc $Rb_xCs_{3-x}C_{60}$ [12]. This state, which connects the insulating and superconducting phases, exhibits a coexistence of localized and itinerant electrons, but the physical origin of this unconventional feature has not been clarified.

An unusual property of fulleride compounds is the effectively negative Hund coupling J produced by anisotropic (Jahn-Teller) phonons [14–22]. In contrast to transition metal (d-electron) systems, which have a positive Hund coupling of the order of 1 eV, the bare Hund coupling in fullerides is much smaller (~30 meV) because of the spatially extended molecular orbitals, so that the screening by phonons can lead to a sign inversion of the effective J [14,15,17].

Theoretically, these systems can be described by a half-filled three-orbital Hubbard model $\mathcal{H} = \mathcal{H}_{\rm kin} + \mathcal{H}_{\rm int}$, where $\mathcal{H}_{\rm kin} = \sum_{\boldsymbol{k}\gamma\gamma'\sigma}(\varepsilon_{\boldsymbol{k}\gamma\gamma'} - \mu\delta_{\gamma\gamma'})c^\dagger_{\boldsymbol{k}\gamma\sigma}c_{\boldsymbol{k}\gamma'\sigma}$ is the kinetic energy of the electrons. The interaction term is of the form

$$\mathcal{H}_{\rm int} = \sum_{i\gamma_1\gamma_2\gamma_3\gamma_4\sigma\sigma'} U_{\gamma_1\gamma_2\gamma_3\gamma_4} c^\dagger_{i\gamma_1\sigma} c_{i\gamma_2\sigma} c^\dagger_{i\gamma_3\sigma'} c_{i\gamma_4\sigma'}, \qquad (1)$$

where $U_{\gamma\gamma\gamma\gamma} = U/2\ (>0)$, $U_{\gamma\gamma\gamma'\gamma'} = U'/2\ (>0)$, $U_{\gamma\gamma'\gamma'\gamma} = U_{\gamma\gamma'\gamma\gamma'} = J/2\ (<0)$ for $\gamma \neq \gamma'$, and the other components are zero. We use the standard parametrization $U' = U - 2J$ valid for isotropic interactions, which results in a $\mathrm{SU}(2) \times \mathrm{SO}(3)$ symmetry in spin-orbital space. The indices $\gamma = 1$, 2, 3 and $\sigma = \uparrow, \downarrow$ represent the three degenerate (t_{1u}) molecular orbitals and spin, respectively. We define the spin and orbital moments by $\boldsymbol{S}_i = \sum_{\gamma\sigma\sigma'} c^\dagger_{i\gamma\sigma}\boldsymbol{\sigma}_{\sigma\sigma'}c_{i\gamma\sigma'}$ and $\tau^\eta_i = \sum_{\gamma\gamma'\sigma} c^\dagger_{i\gamma\sigma}\lambda^\eta_{\gamma\gamma'}c_{i\gamma'\sigma}$, where $\boldsymbol{\sigma}$ is the Pauli matrix and $\lambda^{\eta=1,\ldots,8}$ is the Gell-Mann matrix (see Supplemental Material for more details [23]). In the case of the point-group symmetry I relevant for an isolated fullerene, the

$\eta = 1, 3, 4, 6, 8$ (time-reversal even) components, which play a central role in the following analysis, correspond to the symmetry H, and $\eta = 2, 5, 7$ (time-reversal odd) to T_1 [26]. These are analogs of quadrupole and dipole moments, made from p electrons with angular momentum $\ell = 1$.

To solve the lattice model, we use the dynamical mean-field theory (DMFT) [27,28] in combination with the continuous-time quantum Monte Carlo method [29]. This is a suitable method for three-dimensional systems with strong local correlations, such as fulleride compounds [17]. In DMFT calculations, the relevant information on the kinetic term is the density of states (DOS). We choose $\varepsilon_{\boldsymbol{k}\gamma\gamma'} = \varepsilon_{\boldsymbol{k}}\delta_{\gamma\gamma'}$ and a featureless semicircular DOS defined by $\sum_{\boldsymbol{k}}\delta(\varepsilon - \varepsilon_{\boldsymbol{k}}) = (4/\pi W^2)\sqrt{W^2 - 4\varepsilon^2}$, where W ($\simeq$0.4 eV in fullerides [17]) is used as the unit of energy. This DOS allows us to reveal the generic effect of negative Hund couplings and to discuss phenomena which are independent of material-specific details.

To study the symmetry-breaking transitions, we first truncate the interaction to the density-density components of the form $n_{i\gamma\sigma}n_{i\gamma'\sigma'}$ with $n_{i\gamma\sigma} = c^{\dagger}_{i\gamma\sigma}c_{i\gamma\sigma}$. With this approximation, an anisotropy is introduced in spin and orbital space, and the relevant quantities are S^z, τ^3, and τ^8. Neglecting the spin-flip term $c^{\dagger}_{i\gamma\uparrow}c_{i\gamma\downarrow}c^{\dagger}_{i\gamma'\downarrow}c_{i\gamma'\uparrow}$ ($\gamma \neq \gamma'$) is justified for $J < 0$, since the electrons tend to occupy the same orbital and the interorbital spin degree of freedom is inactive. On the other hand, dropping the pair-hopping term $c^{\dagger}_{i\gamma\uparrow}c^{\dagger}_{i\gamma\downarrow}c_{i\gamma'\downarrow}c_{i\gamma'\uparrow}$ ($\gamma \neq \gamma'$) is motivated by numerical simplifications, and we will discuss the effect of this approximation later. The essential properties are correctly revealed by the simplified model with only density-density-type interactions.

Spontaneous orbital-selective Mott transition.—To demonstrate the existence of the SOSM state, we consider a half-filled system, restrict the interactions to the density-density type, and set $J = -U/4$. This is a large Hund coupling compared to the realistic estimates for fulleride compounds [16], but this parameter choice allows us to clearly reveal the physics with modest computational resources. The results are qualitatively unchanged if we choose smaller Hund couplings, as shown in the Supplemental Material [23]. In the entire parameter regime considered in this study, the ordinary (uniform) orbital moment $\langle \tau^{\eta}_i \rangle$ is zero. To detect the transition to the SOSM state, let us introduce the orbital-dependent double occupancies and kinetic energies $D_\gamma = \sum_i \langle n_{i\gamma\uparrow}n_{i\gamma\downarrow}\rangle/N$ and $K_\gamma = \sum_{\boldsymbol{k}\sigma}\varepsilon_{\boldsymbol{k}}\langle c^{\dagger}_{\boldsymbol{k}\gamma\sigma}c_{\boldsymbol{k}\gamma\sigma}\rangle/N$, with $N = \sum_i 1$, and plot these quantities as a function of U [Figs. 1(a) and 1(b)]. In the interaction range $1 \lesssim U/W \lesssim 1.4$, a spontaneous symmetry breaking is observed, which manifests itself in an orbital imbalance of D_γ and K_γ. If we focus on D_γ and define the composite or two-body orbital moments $\mathcal{T}^{3,8} = \sum_\gamma \lambda^{3,8}_{\gamma\gamma}D_\gamma$, we have $\mathcal{T}^3 = 0$ and $\mathcal{T}^8 > 0$ in the present SOSM state (see also Supplemental Material [23]).

To demonstrate the metallic and insulating characters of the different orbitals, we plot in Fig. 1(c) the purely imaginary self-energies $\Sigma(i\varepsilon_n)$ with $\varepsilon_n = (2n+1)\pi T$ in the SOSM state. Orbital $\gamma = 3$ behaves as a Fermi liquid [$\mathrm{Im}\Sigma(\varepsilon_n \to 0) \to 0$], while the self-energies of the other orbitals diverge at low frequency, indicating a Mott insulating behavior. From studies of the Hubbard model [28], it is known that such a divergence of the self-energy is a characteristic feature of localized or paired electrons [15,30,31]. A schematic illustration for the SOSM state is shown in Fig. 1(d).

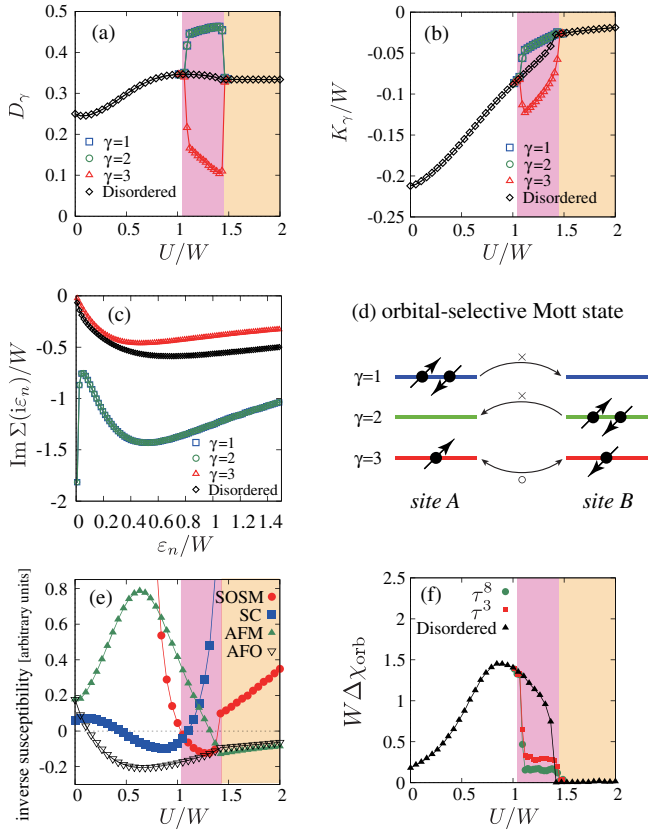

FIG. 1. (a) Orbital-dependent double occupancy and (b) kinetic energy as a function of U at the temperature $T/W = 0.005$ (results for a metallic initial solution). Here we consider only density-density-type interactions. The highlighted regions show the SOSM state (pink) and Mott insulator (orange). (c) Self-energies at $U/W = 1.25$ and $T/W = 0.0025$. (d) Schematic illustration of the SOSM state. (e) Inverse susceptibility for AFM, SC, SOSM, and AFO orders calculated in the normal state without SSB, and (f) local orbital fluctuations at $T/W = 0.005$. The data in panel (e) have been rescaled, since we are interested only in the divergent points.

The half-filled three-orbital system also exhibits conventional forms of symmetry breaking which can be detected by the divergence of the corresponding lattice susceptibilities, as shown in Fig. 1(e). In particular, there is an instability to intraorbital-spin-singlet superconductivity [(SC), order parameter $\langle c^{\dagger}_{i\gamma\uparrow}c^{\dagger}_{i\gamma\downarrow}\rangle$] in the metallic region, and, if we assume a bipartite lattice to simulate bcc fullerides, antiferromagnetic order [(AFM), order parameter $\langle S^z_i \rangle$] is observed in and near the Mott phase. The negative susceptibility for antiferro-orbital order [(AFO),

order parameter $\langle \tau_i^{3,8} \rangle$] indicates the presence of orbital order. This order is, however, not stable against the pair hopping, as discussed later. The SOSM state can also be detected by an odd-frequency susceptibility as shown in the figure, which is explained in the Supplemental Material [23].

By tracking these transition points, we can map out the phase diagram as shown in Figs. 2(c) and 2(d). For comparison, we also sketch the experimental phase diagrams for fulleride compounds in Figs. 2(a) and 2(b). The phase diagram obtained using a metallic initial solution is shown in Fig. 2(c), and the result for an insulating initial solution in Fig. 2(d). A hysteresis behavior is observed near the Mott transition point. In both panels, we indicate the Mott transition points of the system without SSB by black crosses. These critical points delimit the stability regions of the paramagnetic metal (PM) and Mott insulator (MI), respectively, and end at a critical end point (CEP) at a finite temperature. We note that it is difficult to accurately determine the metal-insulator transition points, since tiny numerical errors destroy the metastable insulating state near the boundary.

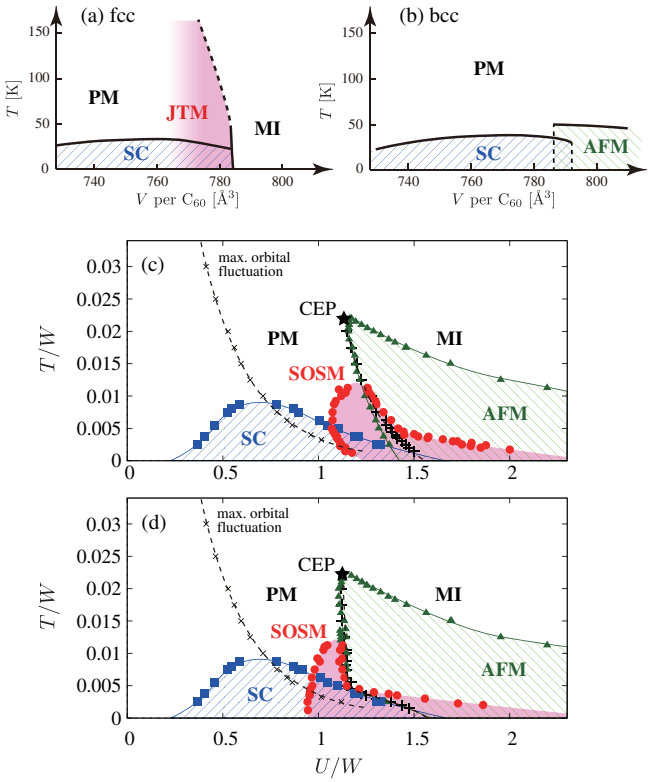

FIG. 2. Sketches of the experimental phase diagrams for (a) fcc and (b) bcc fullerides based on Refs. [11,12]. Panels (c) and (d) show the phase diagrams of the three-orbital Hubbard model for density-density interactions and negative Hund coupling $J = -U/4$, calculated using a metallic and insulating initial solution, respectively. The boundary of the SOSM phase has been determined from the points where the order parameter becomes finite, while the other boundaries are determined from the divergent points of the corresponding susceptibilities. Here we do not consider the coexistence of two different orders. In overlapping regions, the energetically favorable ordered state will dominate.

The SOSM state is stabilized near the Mott phase, while SC appears in the lower-U region. The transition into the SOSM and AFM phases is of first order: If the U dependence is scanned from the metallic side, the instabilities occur at different interaction values than if the calculation is started on the Mott insulator side. The results also apply to the fcc lattice case if we neglect the AFM phase, which is suppressed by geometrical frustration. Comparing the simulation results with the experimental phase diagrams sketched in Figs. 2(a) and 2(b), we see that our model captures the characteristic properties of the fulleride compounds, including the dome shape of the SC region, and the Jahn-Teller metal, which is here identified as a SOSM state. Although the Jahn-Teller metal has been observed only in the fcc system, our results suggest that it can be stabilized also on the bcc lattice. At a sufficiently low temperature, we observe the metal-insulator transition *inside* the SOSM phase. However, this insulating SOSM state might not be detectable experimentally, since we expect magnetic order at large U and at low temperatures.

The SC dome is related to the local orbital fluctuations defined by $\Delta\chi_{\rm orb} = \int_0^\beta d\tau [\langle \tau_i^\eta(\tau)\tau_i^\eta\rangle - \langle \tau_i^\eta(\beta/2)\tau_i^\eta\rangle]$ with $\eta = 3$ or 8, where the second term is the long-(imaginary-)time correlator and $\beta = 1/T$. As shown in Fig. 1(f), these fluctuations reach a maximum at an interaction considerably lower than the Mott critical value. The temperature dependence of these maxima yields the crossover line marked with diagonal crosses in Figs. 2(c) and 2(d). Evidently, the SC dome is peaked in the region of maximum orbital fluctuations. In this sense, the intraorbital spin-singlet pairing in fulleride compounds is the negative-J analog of the recently discussed fluctuating local spin-moment-induced spin-triplet superconductivity in multiorbital systems with $J > 0$ [32,33]. More explicitly, the originally repulsive intraorbital interaction U can become attractive by considering the second-order perturbation contribution,

$$\tilde{U} \simeq U - 4U'(U' + |J|)\chi_{\rm loc} + O(U^3), \qquad (2)$$

as a result of enhanced local orbital fluctuations $\chi_{\rm loc}$ (see Refs. [32,34]). In the SOSM state, these local orbital fluctuations are suppressed, as shown in Fig. 1(f), and the results for the $\eta = 8$ and $\eta = 3$ components differ. Although this indicates a suppression of SC, with the pair-hopping term the fluctuations partly remain and may even be enhanced, as discussed below.

Effect of pair hopping.—To illustrate the effect of the spin-flip and pair-hopping terms, which recover the continuous rotational symmetry in spin and orbital space, we present results for a Hund coupling of $J = -U/10$. Figure 3 shows the orbital-dependent double occupancies and inverse susceptibilities for the AFM, AFO, SC, and SOSM states. These quantities are the same as previously discussed for the density-density case in Fig. 1. As shown in Fig. 3(a), the double occupancies (and also kinetic energies) become orbital dependent spontaneously for a range of interaction values near the Mott transition point.

Even though we choose here a smaller value of $|J|$ than in the density-density interaction case, the widths of the SOSM regions in Figs. 1 and 3 are almost identical. This demonstrates that the pair hopping stabilizes the SOSM state. A similar conclusion applies to SC, which covers a wider U region than in the density-density case. We have also confirmed that the SOSM state can be stabilized for even smaller and more realistic [16] $|J|$ values, such as $J = -0.03U$ (see Supplemental Material [23]).

The comparison of Figs. 3(c) and 1(e) shows that the AFO order is suppressed due to the pair-hopping term, which mixes different orbital states and washes out the orbital moments. Hence, the AFO order in the model with only density-density-type interactions is an artifact of the missing pair-hopping term. Although there is a region where the AFO susceptibility is negative, this region is away from the Mott transition point.

As mentioned above, the spin-singlet pairing is strongly enhanced by the pair hopping, which means that it is underestimated in the model with only density-density interactions. This can be understood as follows: In the SC phase, the negative pair-hopping term can be decoupled as $|J|\sum_i c^\dagger_{i1\uparrow} c^\dagger_{i1\downarrow} \langle c_{i2\uparrow} c_{i2\downarrow}\rangle + \text{H.c.} + \cdots$, which shows that condensation energy for pairing is gained at the static mean-field level, and it should increase the pair amplitude (and also T_c). In the SOSM state, orbital fluctuations of the τ^8 moment are suppressed but those for τ^3 are enhanced, as shown in Fig. 3(d). This is in contrast to Fig. 1(f). Thus, in the rotationally invariant case, the orbital fluctuations persist and can help SC inside the SOSM state, compared to the case without pair hopping. We note that it has been demonstrated that an imbalance of the Coulomb interaction, which produces an effect similar to the symmetry-breaking field in the SOSM state, can enhance the superconductivity in the weak coupling regime [22]. It is also notable that $\Delta\chi_{\text{orb}}$ in the Mott insulator regime is enhanced compared to Fig. 1(f) due to the pair hopping.

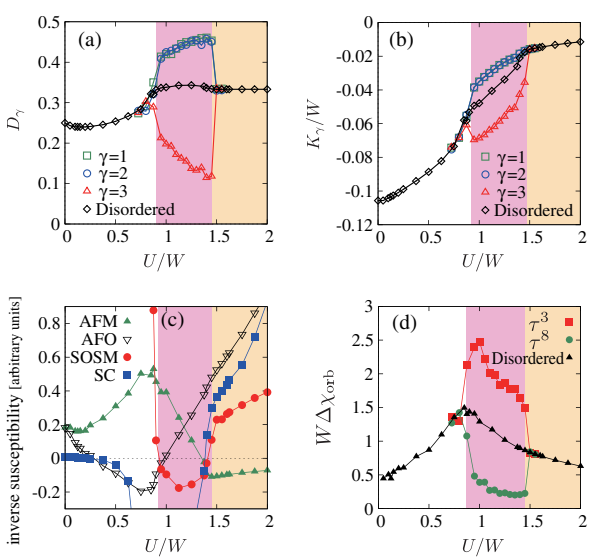

FIG. 3. Results analogous to Fig. 1, but for the model with full interaction including pair hopping. Here $J = -U/10$ and $T/W = 0.005$.

We also comment on the origin of the SOSM state. The fluctuation of the composite moment $\mathcal{T}^8 = (D_1 + D_2 - 2D_3)/\sqrt{3}$ at low temperatures can be captured already in the atomic limit with $U \to \infty$ (see Supplemental Material for more details [23]). Hence, the composite moment $\mathcal{T}^8$ tends to order in the lattice environment and should be regarded as the primary order parameter. On the other hand, the orbital imbalance of the kinetic energies, which appears simultaneously with $\mathcal{T}^8 \neq 0$, may be regarded as a secondary effect. This picture is further supported by the fact that the phase boundary of the (insulating) SOSM state has a long tail at large U as shown in Figs. 2(c) and 2(d), indicating the relevance of the $U \to \infty$ limit.

Diagonal odd-frequency order.—So far, we have characterized the SOSM state by the static orbital imbalance in the double occupancy and/or kinetic energy. Here we show that both pictures are captured simultaneously by the time-dependent quantity

$$T^\eta(\tau) = \sum_{i\gamma\gamma'\sigma} \langle c^\dagger_{i\gamma\sigma} \lambda^\eta_{\gamma\gamma'} c_{i\gamma'\sigma}(\tau)\rangle, \tag{3}$$

which is odd with respect to time, since $T^\eta(0)$ is an ordinary orbital moment and thus vanishes. If $T^\eta(\tau)$ becomes finite, it describes the orbital SSB. To obtain a static representation of the order, we expand $T^\eta(\tau)$ with respect to imaginary time:

$$T^\eta(\tau) = T^\eta_{\text{even}} + T^\eta_{\text{odd}}\tau + O(\tau^2), \tag{4}$$

with a vanishing ordinary order parameter: $T^\eta_{\text{even}} = 0$. The first-order contribution (or "odd-frequency" component) T^η_{odd}, which characterizes the odd time dependence of the order parameter of the SOSM state, may be regarded as a generalized orbital moment. The explicit form is given by

$$T^8_{\text{odd}} = \sum_\gamma \lambda^8_{\gamma\gamma}(K_\gamma + 2UD_\gamma) + (\text{other terms}), \tag{5}$$

where the "other terms" originate from the interorbital interactions (U' and J). As seen in Eq. (5), T^8_{odd} incorporates the orbital-dependent kinetic energies and double occupancies and provides an alternative characterization of the SOSM state. In a manner analogous to ordinary orders, the corresponding instability can be detected by looking for the divergence of the odd-frequency orbital susceptibility [25], as shown in Figs. 1(e) and 3(c). Hence, this concept provides a convenient tool for detecting the composite ordered phases.

Summary and outlook.—Orbital-selective Mott states have been previously discussed in systems with an originally broken orbital symmetry, due to either orbital-dependent bandwidths [35–38] or crystal-field splittings [39]. The orbital-selective states revealed in this work are of a fundamentally different nature, since they correspond to a *spontaneous* symmetry breaking in an orbitally degenerate system [40]. This exotic state of matter is characterized by an unusual order parameter, i.e., an orbital-dependent double occupancy (composite order parameter) and/or kinetic

energy. These physical quantities naturally appear in the time-dependent orbital moment with odd time dependence, which allows us to interpret the present order as an odd-frequency order. This concept, which has first been introduced as odd-frequency superconductivity, is generalized here to the diagonal-order version. Our work demonstrates the existence of this unconventional order in multiorbital Hubbard systems with negative Hund coupling and provides strong evidence that it is actually realized in fulleride compounds, in the form of the Jahn-Teller metal phase.

The SOSM states discussed here appear in half-filled multiorbital systems with an odd number (> 1) of orbitals. In the two-orbital case, the phenomenon cannot be observed, because the pairing of electrons will simply lead to a paired Mott insulator in all orbitals. If an odd number of electrons is present, as in the three-orbital case and also in half-filled five- or seven-orbital systems, there will always be at least one unpaired electron left, which can support metallicity.

There exist several kinds of degenerate SOSM states, which are related by symmetry. It should thus be possible to switch from one SOSM phase to another by applying pressure or electric fields or by photoexcitation. The experimental detection and control of these exotic ordered states will be an interesting future challenge. Since the different SOSM phases can be distinguished by their anisotropic conductivity, a reliable switching protocol could pave the way to energy-efficient and fast memory devices.

The authors thank A. Koga and Y. Nomura for valuable discussions. S. H. acknowledges financial support from Japan Society for Promotion of Science (JSPS) KAKENHI Grants No. 13J07701 and No. 16H04021, and P. W. support from the European Research Council Starting Grant No. 278023. The authors benefited from the Japan-Swiss Young Researcher Exchange Program 2014 coordinated by JSPS and State Secretariat for Education, Research and Innovation (Switzerland). The numerical calculations have been performed using the supercomputer at Institute for Solid State Physics (the University of Tokyo), the BEO04 cluster at the University of Fribourg, and the CET-7 cluster at CEMS (RIKEN).

[1] V. L. Berezinskii, JETP Lett. **20**, 287 (1974).
[2] T. R. Kirkpatrick and D. Belitz, Phys. Rev. Lett. **66**, 1533 (1991).
[3] A. Balatsky and E. Abrahams, Phys. Rev. B **45**, 13125 (1992).
[4] V. J. Emery and S. Kivelson, Phys. Rev. B **46**, 10812 (1992).
[5] A. F. Hebard, M. J. Rosseinsky, R. C. Haddon, D. W. Murphy, S. H. Glarum, T. T. M. Palstra, A. P. Ramirez, and A. R. Kortan, Nature (London) **350**, 600 (1991).
[6] M. J. Rosseinsky, A. P. Ramirez, S. H. Glarum, D. W. Murphy, R. C. Haddon, A. F. Hebard, T. T. M. Palstra, A. R. Kortan, S. M. Zahurak, and A. V. Makhija, Phys. Rev. Lett. **66**, 2830 (1991).
[7] K. Holczer, O. Klein, S. Huang, R. B. Kaner, K. Fu, R. L. Whetten, and F. Diederich, Science **252**, 1154 (1991).
[8] K. Tanigaki, T. W. Ebbesen, S. Saito, J. Mizuki, J. S. Tsai, Y. Kubo, and S. Kuroshima, Nature (London) **352**, 222 (1991).
[9] R. M. Fleming, A. P. Ramires, M. J. Rosseinsky, D. W. Murphy, R. C. Haddon, S. M. Zahurak, and A. V. Makhija, Nature (London) **352**, 787 (1991).
[10] C. M. Varma, J. Zaanen, and K. Raghavachari, Science **254**, 989 (1991).
[11] Y. Takabayashi, A. Y. Ganin, P. Jeglič, D. Arčon, T. Takano, Y. Iwasa, Y. Ohishi, M. Takata, N. Takeshita, K. Prassides, M. J. Rosseinsky, Science **323**, 1585 (2009).
[12] R. H. Zadik, Y. Takabayashi, G. Klupp, R. H. Colman, A. Y. Ganin, A. Potočnik, P. Jeglič, D. Arčon, P. Matus, K. Kamarás, Y. Kasahara, Y. Iwasa, A. N. Fitch, Y. Ohishi, G. Garbarino, K. Kato, M. J. Rosseinsky, K. Prassides, Sci. Adv. **1**, e1500059 (2015).
[13] M. Mitrano, A. Cantaluppi, D. Nicoletti, S. Kaiser, A. Perucchi, S. Lupi, P. Di Pietro, D. Pontiroli, M. Riccò, S. R. Clark, D. Jaksch, and A. Cavalleri, Nature (London) **530**, 461 (2016).
[14] M. Fabrizio and E. Tosatti, Phys. Rev. B **55**, 13465 (1997).
[15] M. Capone, M. Fabrizio, C. Castellani, and E. Tosatti, Science **296**, 2364 (2002).
[16] Y. Nomura, K. Nakamura, and R. Arita, Phys. Rev. B **85**, 155452 (2012).
[17] Y. Nomura, S. Sakai, M. Capone, and R. Arita, Sci. Adv. **1**, e1500568 (2015).
[18] Y. Nomura and R. Arita, Phys. Rev. B **92**, 245108 (2015).
[19] M. Capone, M. Fabrizio, C. Castellani, and E. Tosatti, Rev. Mod. Phys. **81**, 943 (2009).
[20] Y. Nomura, S. Sakai, M. Capone, and R. Arita, J. Phys. Condens. Matter **28**, 153001 (2016).
[21] S. Hoshino and P. Werner, Phys. Rev. B **93**, 155161 (2016).
[22] M. Kim, Y. Nomura, M. Ferrero, P. Seth, O. Parcollet, and A. Georges, Phys. Rev. B **94**, 155152 (2016).
[23] See Supplemental Material at http://link.aps.org/supplemental/10.1103/PhysRevLett.118.177002 for detailed information of orbital moments and for additional numerical data, which includes Refs. [16,22,24,25].
[24] M. Jarrell, H. Pang, and D. L. Cox, Phys. Rev. Lett. **78**, 1996 (1997).
[25] S. Hoshino, J. Otsuki, and Y. Kuramoto, Phys. Rev. Lett. **107**, 247202 (2011).
[26] S. Saito and A. Oshiyama, Phys. Rev. Lett. **66**, 2637 (1991).
[27] Y. Kuramoto, in *Theory of Heavy Fermions and Valence Fluctuations*, edited by T. Kasuya and T. Saso (Springer, New York, 1985), p. 152.
[28] A. Georges, G. Kotliar, W. Krauth, and M. J. Rozenberg, Rev. Mod. Phys. **68**, 13 (1996).
[29] P. Werner and A. J. Millis, Phys. Rev. B **74**, 155107 (2006).
[30] R. Micnas, J. Ranninger, and S. Robaszkiewicz, Rev. Mod. Phys. **62**, 113 (1990).
[31] A. Koga and P. Werner, Phys. Rev. B **91**, 085108 (2015).
[32] S. Hoshino and P. Werner, Phys. Rev. Lett. **115**, 247001 (2015).
[33] K. Steiner, S. Hoshino, Y. Nomura, and P. Werner, Phys. Rev. B **94**, 075107 (2016).

[34] K. Inaba and S. I. Suga, Phys. Rev. Lett. **108**, 255301 (2012).
[35] V. I. Anisimov, I. A. Nekrasov, D. E. Kondakov, T. M. Rice, and M. Sigrist, Eur. Phys. J. B **25**, 191 (2002).
[36] A. Koga, N. Kawakami, T. M. Rice, and M. Sigrist, Phys. Rev. Lett. **92**, 216402 (2004).
[37] K. Inaba and A. Koga, Phys. Rev. B **73**, 155106 (2006).
[38] L. de' Medici, S. R. Hassan, M. Capone, and X. Dai, Phys. Rev. Lett. **102**, 126401 (2009).
[39] P. Werner and A. J. Millis, Phys. Rev. Lett. **99**, 126405 (2007).
[40] A detection of collective excitation modes associated with the spontaneous orbital symmetry breaking could provide experimental evidence for the present SOSM phase.